@BoneJointRes

Enhancement of hyaline cartilage and subchondral bone regeneration in a rat osteochondral defect model through focused extracorporeal shockwave therapy

modulation of transforming growth factor-beta and bone morphogenetic proteins-2, -3, -4, -5, and -7 expression

From Kaohsiung Chang Gung Memorial Hospital, Kaohsiung, Taiwan

Cite this article:
Bone Joint Res 2024;13(7):
342–352.

DOI: 10.1302/2046-3758.
137.BJR-2023-0264.R2

Correspondence should be sent to Jai-Hong Cheng
cjh1106@cgmh.org.tw

J-H. Cheng,[1,2,3] S-W. Jhan,[1,4] P-C. Chen,[5] S-L. Hsu,[1,4] C-J. Wang,[1,4] D. Moya,[6] Y-N. Wu,[7] C-Y. Huang,[1,2] W-Y. Chou,[1,4] K-T. Wu[1,4]

[1]Center for Shockwave Medicine and Tissue Engineering, Kaohsiung Chang Gung Memorial Hospital and Chang Gung University College of Medicine, Kaohsiung, Taiwan
[2]Department of Medical Research, Kaohsiung Chang Gung Memorial Hospital and Chang Gung University College of Medicine, Kaohsiung, Taiwan
[3]Department of Leisure and Sports Management, Cheng Shiu University, Kaohsiung, Taiwan
[4]Department of Orthopedic Surgery, Kaohsiung Chang Gung Memorial Hospital and Chang Gung University College of Medicine, Kaohsiung, Taiwan
[5]Department of Physical Medicine and Rehabilitation, Kaohsiung Chang Gung Memorial Hospital, College of Medicine, Chang Gung University, Kaohsiung, Taiwan
[6]Buenos Aires British Hospital, Buenos Aires, Argentina
[7]School of Medicine, Fu Jen Catholic University, New Taipei City, Taiwan

Aims

To explore the efficacy of extracorporeal shockwave therapy (ESWT) in the treatment of osteochondral defect (OCD), and its effects on the levels of transforming growth factor (TGF)-β, bone morphogenetic protein (BMP)-2, -3, -4, -5, and -7 in terms of cartilage and bone regeneration.

Methods

The OCD lesion was created on the trochlear groove of left articular cartilage of femur per rat (40 rats in total). The experimental groups were Sham, OCD, and ESWT (0.25 mJ/mm^2, 800 impulses, 4 Hz). The animals were euthanized at 2, 4, 8, and 12 weeks post-treatment, and histopathological analysis, micro-CT scanning, and immunohistochemical staining were performed for the specimens.

Results

In the histopathological analysis, the macro-morphological grading scale showed a significant increase, while the histological score and cartilage repair scale of ESWT exhibited a significant decrease compared to OCD at the 8- and 12-week timepoints. At the 12-week follow-up, ESWT exhibited a significant improvement in the volume of damaged bone compared to OCD. Furthermore, immunohistochemistry analysis revealed a significant decrease in type I collagen and a significant increase in type II collagen within the newly formed hyaline cartilage following ESWT, compared to OCD. Finally, SRY-box transcription factor 9 (SOX9), aggrecan, and TGF-β, BMP-2, -3, -4, -5, and -7 were significantly higher in ESWT than in OCD at 12 weeks.

Conclusion

ESWT promoted the effect of TGF-β/BMPs, thereby modulating the production of extracellular matrix proteins and transcription factor involved in the regeneration of articular cartilage and subchondral bone in an OCD rat model.

Bone & Joint Research

Article focus

- The focus of this study was to investigate the effectiveness of extracorporeal shockwave therapy (ESWT) as a treatment for osteochondral defect (OCD) and its impact on the expression levels of transforming growth factor (TGF)-β, as well as bone morphogenetic protein (BMP)-2, -3, -4, -5, and -7, which are associated with cartilage and bone regeneration.
- ESWT reduced fibrosis formation to promote cartilage repair, and also stimulated bone regeneration to exhibit a typical pattern of bottom-to-top and edge-to-centre growth in OCD lesion.

Key messages

- ESWT enhanced hyaline cartilage formation, as indicated by a significant increase in type II collagen expression and a decrease in type I collagen. This suggests that ESWT promotes the development of a more cartilage-like matrix in the repaired tissue, contributing to better functional outcomes.
- The study highlights the time-dependent effects of ESWT. The improvements in histopathological grading and volume of damaged bone are more pronounced at the 12-week follow-up, indicating that the benefits of treatment become more evident with time.
- ESWT modulates the expression of important factors like SRY-box transcription factor 9 (SOX9), aggrecan, TGF-β, and various BMPs. These factors play a critical role in tissue regeneration, indicating that ESWT may orchestrate a favourable microenvironment for effective healing.

Strengths and limitations

- This study has used a rat model to mimic human OCD lesions, enhancing the translational relevance of the findings. The animal model allows for controlled experimentation and a deeper exploration of the mechanisms underlying the effects of ESWT in modulation of growth factors and key cartilage matrix proteins.
- While the study observes changes in TGF-β and BMPs expression, it does not delve deeply into the underlying mechanisms of how ESWT precisely influences these pathways. Further mechanistic studies could enhance understanding of the treatment.

Introduction

An osteochondral defect (OCD) refers to a localized injury within a joint, predominantly observed in the knee, which involves damage to both the articular cartilage and subchondral bone.[1] OCD often causes pain, swelling, and catching in the joint. Severe OCD without treatment often causes fibrous tissue formation and degenerative changes in the surrounding cartilage tissues and bones, resulting in arthritis in the knee.[2] Surgical treatments are common clinical treatments for cartilage defects including chondroplasty, microfracture, fixation, osteochondral autograft transplant, osteochondral allograft transplant, autologous matrix induced-chondrogenesis, and autologous chondrocyte implantation.[3,4] In addition, many researchers have developed other methods to promote the healing process of full-thickness articular cartilage defects. Several techniques and procedures have been studied to restore damaged cartilage, including cell-based therapy, small molecules, tissue engineering, and nonoperative management.[5,6] While some of these procedures have achieved limited success, none have shown universal results and require further study.

Extracorporeal shockwave therapy (ESWT) is a noninvasive, physical stimulation and acoustic wave therapy that has been used to treat various musculoskeletal diseases, including osteoarthritis, plantar fasciitis of the heel, calcific tendonitis of the shoulder, lateral epicondylitis of the elbow, avascular necrosis, and nonunion of long bone fractures.[7,8] In animal experiments, ESWT has been observed to stimulate the growth of new blood vessels and enhance the production of factors that promote tissue repair and regeneration.[8,9] Numerous other studies have demonstrated that ESWT initiates a mechanotransduction process that induces biological responses, including angiogenesis at cellular and molecular levels, in tissue repair.[10,11]

Evidence shows that physical stimulations can promote cartilage and bone regeneration, including ESWT, which promotes articular cartilage healing and has a chondroprotective effect by inducing transforming growth factor (TGF)-β and bone morphogenetic protein (BMP)-2, preventing knee osteoarthritis and OCD development.[12,13] In vivo, ESWT promotes the formation of hyaline-like cartilage repair tissue in microfracture holes more than microfracture alone in a rabbit model.[14] Another study shows that ESWT improves cartilage health by regulating matrix metalloproteinase -1, -3, -13, and tissue inhibitors of metalloproteinase-1 levels in cartilage, and altering subchondral bone metabolism.[15] In addition, ESWT can influence the metabolic processes involving glycosaminoglycan in chondrocytes within equine articular cartilage.[16] However, the precise mechanisms through which ESWT promotes the regeneration of cartilage and bone in OCD are not yet fully understood, particularly in relation to the stimulation of TGF-β, BMPs, transcription factors, and extracellular proteins.

ESWT does not seem to cause structural damage to the cartilage in joints; however, it affects the viability of chondrocytes and the permeability of their membranes.[9,17,18] Furthermore, ESWT caused dose-dependent changes in the intervertebral end plate and stimulated angiogenesis at the cartilage end plate in rabbits.[19] Some studies indicate that ESWT does not cause injury to the joint cartilage of growing rabbits.[17,20] ESWT has been shown to benefit cartilage repair in animals;[21,22] however, the specific role of TGF-β/BMPs in the repair of OCD following ESWT remains unknown. This study aims to examine and understand how TGF-β/BMPs are expressed to recover hyaline cartilage and subchondral bone during the regeneration process following focused ESWT in an OCD rat model.

Methods

Animals

Rat maintenance and experimental procedures were approved by Kaohsiung Chang Gung Memorial Hospital Animal Ethical and Care Committee (Approval Number: 2017111401). We have included an ARRIVE checklist to show that we have conformed to the ARRIVE guidelines. A total of 90 Sprague-Dawley rats (150 g to 200 g, six weeks old) were purchased from BioLASCO (Taiwan), housed at 23°C ± 1°C with a 12-hour

light and dark cycle, and provided with food and water. All rats were allowed to adjust to the new environment for one week before surgery.

Experimental design

The sample size of ten rats in each group was calculated with a power of 80%, an α level of 0.05, and a 20% dropout rate, based on a two-tailed test. All rats were randomized to be divided into three groups and designated as Sham (n = 10), OCD (n = 40), and ESWT (n = 40) for the experiments at different timepoints (Supplementary Figure a). In the Sham group, parapatellar skin incisions without defects were created on the medial sides of the left knee without surgery and ESWT (Figure 1a and Supplementary Figure ba). In the OCD group, the defects were created in the trochlear groove of the left femur without receiving ESWT (Supplementary Figure bb, bc, and bd). In the ESWT group, the defects were created on the trochlear groove of the left femur and received focused shockwaves (SW) (0.25 mJ/mm^2 with 800 impulses, 4 Hz, Supplementary Figure be). All animals were maintained under standard sterile conditions throughout the surgical procedure, and postoperatively they received a five-day course of ampicillin (25 mg/kg) and ketorolac (1 mg/kg/day) to prevent infection and manage pain, respectively. The animals were euthanized at two, four, eight, and 12 weeks post-treatment for OCD and ESWT (each timepoint had n = 10). The Sham rats were euthanized at 12 weeks post-treatment; their left knee was collected and kept for further analysis.

OCD model and focused SW application

The rats were anaesthetized with xylazine (10 mg/kg) and Zoletil (20 mg/kg). The OCD was created by drilling an area with 0.50 mm diameter for depth and 2 mm diameter for width on the left trochlear groove of the left rat knee (Supplementary Figure bb, bc, and bd). In ESWT, focused shockwaves were applied one week after surgery. A radiograph and ultrasound guidance (Toshiba Corporation, Japan) were first performed to mark the location and survey the lesion size before undertaking focused ESWT using DUOLITH SD1 (Storz Medical, Switzerland) (Supplementary Figure be and bf). The animals were sedated with isoflurane and received ESWT. For a single session, 800 impulses of focused shockwaves at 0.25 mJ/mm^2 energy flux density, 4 Hz, were directly applied to the defective area of each animal. After ESWT, the veterinarian took care of the animals until sacrifice for the experiments.

Gross morphological grading and micro-CT analysis

In the femurs of each group, the pathological OCD area was examined and photographed for evaluation according to the International Cartilage Repair Society (ICRS) macroscopic assessment scale (Figure 1a).[25] The distal part of the femur with OCD was scanned by the micro-CT scanner (SkyScan 1076, Belgium) with an isotopic pixel size at 36 × 36 × 36 μm and radiograph voltage of 100 kV. Image reconstructions were performed, and a series of planar transverse grayscale images were generated using NRecon software (SkyScan) as previously described.[17] The region of interest in the bone morphometry was selected by a semiautomatic contouring method, and it was segmented into binary images using the SkyScan CT-Analyzer programme (Figure 1a). Consequently, the percentage of bone volume fraction (BV/TV%) was used for bone recovery analysis.

Pineda's histological score and Wakitani's cartilage repair score

Knee specimens were fixed in 4% formaldehyde for 48 hours and decalcified in 10% ethylenediaminetetraacetic acid (EDTA) for a month. Tissue sections of 5 μm each were embedded in paraffin, using Pineda's histological scoring system for haematoxylin and eosin (HE) staining.[23] Pineda's histological scoring system employs a scale ranging from 0 (complete regeneration) to 14 (no repair). The assessment involves quantifying tissue damage levels, categorized by defect filling, restoration of the osteochondral junction, matrix staining, and cell appearance. A higher total score indicates more severe histological damage. For cartilage repair analysis, Safranin-O staining was performed according to a previously published protocol,[26] and specimens were graded using Wakitani's system based on cartilage cell morphology, matrix stain intensity, cartilage surface regularity, cartilage thickness, and adjacent cartilage integration, which are indicators of cartilage recovery conditions.[24]

Immunohistochemical analysis

The tissue sections were first treated with xylene to remove paraffin, then hydrated using graded ethanol. Next, they were subjected to peroxide- and protein-blocking reagents. Specific antibodies for collagen I were used to immunostain sections of the specimens overnight at a dilution of 1:200 (Cell Signalling), for collagen II at 1:200 dilution, for SRY-box transcription factor 9 (SOX9) at 1:100, for aggrecan at 1:50 (Abcam, USA), for TGF-β at 1:100 (Abcam, USA), for BMP-2, -3, -4, and -7 at 1:200 (Abcam, USA), and for BMP-5 at 1:100 (Invitrogen; Thermo Fisher Scientific, USA) to identify the biomarkers of chondrogenesis and bone regeneration. The kit provided goat anti-rabbit horseradish peroxidase-conjugated and 3',3'-diaminobenzendine to show immunoreactivity in the specimens. Using a Zeiss Axioskop 2 Plus microscope (Carl Zeiss, Germany), the immunoactivities of cells in five randomly selected areas in three sections of the same specimen were quantified. A charge-coupled device camera (Media Cybernetics, USA) was used to capture all images of each specimen, and ImageJ (National Institutes of Health (NIH), USA) was used to analyze the images. ImagePro analysis software (Media Cybernetics, USA) was used to obtain the percentage of positively stained cells. For immunohistochemical (IHC) staining intensity, images were analyzed using ImageJ IHC profiler plugin (NIH) analysis software obtaining percent of positively staining cells for the cartilage (Supplementary Table i). There were five to six random areas of IHC bone marrow images were taken on the upper cross-sectional area of a slide around the OCD sites. The intensities of bone marrow cell staining were determined using the colour deconvolution function to filter out 3,3' -diaminobenzidine (DAB) staining slides (Supplementary Table ii).[27,28]

Statistical analysis and image processing

All data were analyzed by SPSS (version 17.0; SPSS, USA) and were represented as mean and standard deviation (SD). The Mann-Whitney U test was used for group comparisons of ranking data (non-normal distribution). A two-tailed paired

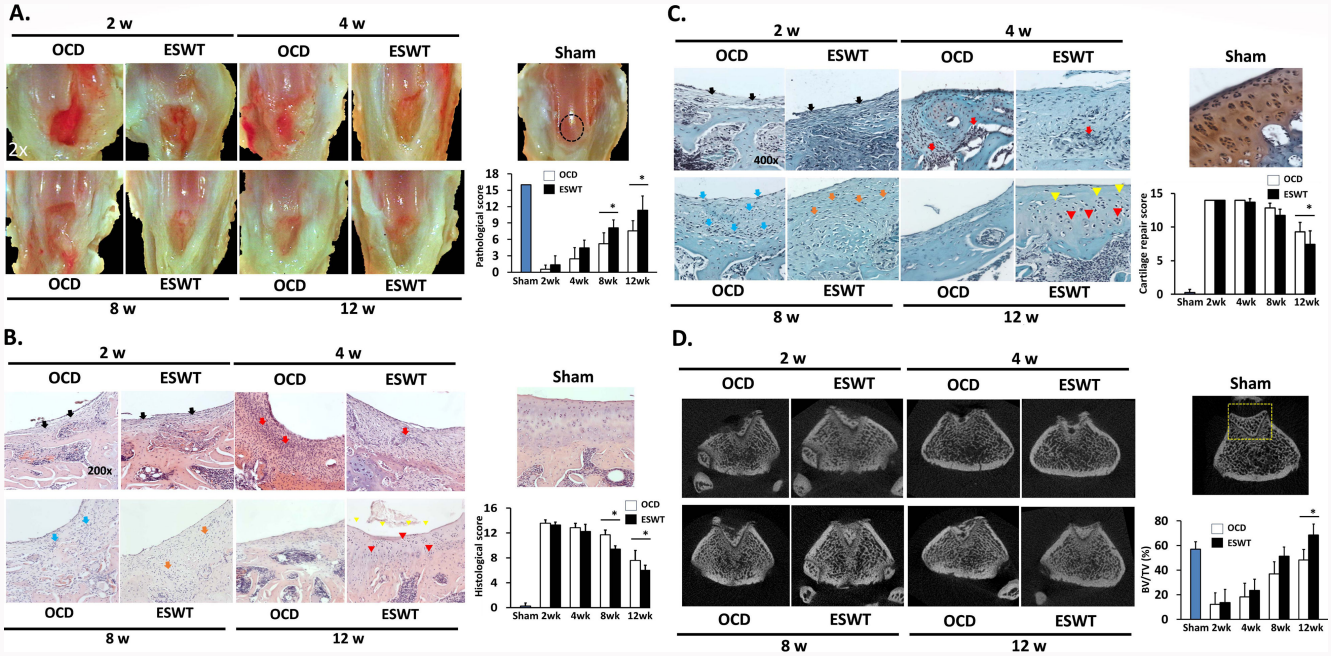

Fig. 1

The evaluated tissue profiles from the Sham, osteochondral defect (OCD), and extracorporeal shockwave therapy (ESWT) groups at two, four, eight, and 12 weeks. a) Macroscopic changes in each group are observed and quantified using International Cartilage Repair Society pathological scores (magnification: ×2). b) Histological changes are examined through haematoxylin and eosin staining in each group, with scores calculated using Pineda's histological scoring system (magnification: ×200).[23] c) Cartilage regeneration is assessed using Safranin-O staining in each group, and scores are determined using Wakitani's cartilage repair scoring system (magnification: ×400).[24] d) Micro-CT images and analysis are conducted to evaluate new bone formation, quantified by percentage of bone volume fraction (BV/TV%). *p < 0.05 (Mann-Whitney U test), comparing between OCD and ESWT groups.

t-test was used for group comparisons of numerical data. Differences were considered statistically significant at $p < 0.05$. The fibre and collagen loci were processed and imaged by ImageJ and CT-Fire software (2.0 β version, University of Wisconsin-Madison), all according to previously published instructions.[29,30] In brief, in the HE stain images, ImageJ first processed colour separation via colour deconvolution for the separation of the red, green, and blue components. The green component was identified as the patterns of collagen fibre threads. Therefore, their orientations were determined by CT-Fire software. Consequently, the fibre collagen thread locus was imaged by ImageJ via the threshold function.

Results

Macro-morphological analysis

In this study, we first examined the macro-morphological changes in knee injury lesions over time (2, 4, 8, and 12 weeks) following treatment in OCD and ESWT groups (Figure 1a). Initially, at two weeks, both groups exhibited open wounds, redness, structural disruptions, and fissures, covered by fibrous tissue. However, by four weeks, the ESWT group displayed smoother fibrous tissue coverage compared to the partially open wounds in the OCD group. Over time, both groups saw increased yellowish fibrous tissue coverage and reduced irregularities. Remarkably, at 12 weeks, the ESWT-treated lesions showed complete coverage with glistening white cartilage-like tissue, while wound margins were still visible in both groups. ESWT significantly improved the pathological scores compared to OCD at eight weeks ($p < 0.05$, Mann-Whitney U test) and 12 weeks ($p < 0.05$, Mann-Whitney U test) post-treatment (Figure 1a).

ESWT enhanced hyaline cartilage regeneration

We conducted Pinda's histological analysis using HE staining to visualize the general tissue structure, and the Walkitani's cartilage score using Safranin-O staining visualize proteoglycan in cartilage, in the Sham, OCD, and ESWT groups from two to 12 weeks (Figures 1b and 1c and Supplementary Figure c). In Sham, the cartilage showed smooth surface and healthy chondrocytes in a typical oval shape, which arranged regularly, and divided chondrocytes were frequently observed. At two weeks, both OCD and ESWT groups had thin fibrous tissue layers covering the lesion. By four weeks, the OCD group showed inflammation with lymphocyte hyperplasia, while ESWT reduced inflammation. At eight weeks, the OCD group had fibrous tissue and elongated fibroblasts, while the ESWT group induced the formation of fibrochondrocytes. At 12 weeks, the ESWT group exhibited chondroblast and chondrocytes compared with the OCD group.

Pineda's histological score significantly favoured ESWT over OCD at eight weeks ($p < 0.05$, Mann-Whitney U test) (Figure 1b). However, at 12 weeks, both groups showed rapid improvements in wound recovery and margin integration, with no significant difference. ESWT enhanced wound healing compared to OCD. For the cartilage score, no significant differences were seen at two, four, and eight weeks. At 12 weeks, ESWT significantly reduced the score compared to OCD ($p < 0.05$, Mann-Whitney U test) (Figure 1c). ESWT promoted cartilage self-recovery and proteoglycan structure

formation within the lesion, indicating its beneficial effects on cartilage repair.

ESWT improved bone recovery in OCD lesions

In the repair of OCD lesions, bone regeneration was illustrated by using micro-CT imaging (Figure 1d). Notably, the micro-CT images were particularly focused on the regions of epiphyseal compartment at their transverse positions (Figure 1d). At two and four weeks, both OCD and ESWT groups showed extensive bone damage and erosions at the lesion sites, with thickened osseous lining toward the femoral grooves and cystic structures. By eight weeks, ESWT displayed intense whitish osseous tissues, indicating new bone formation, while the OCD group still had cysts and erosions. At 12 weeks, ESWT-treated bones exhibited dense, smooth osseous tissues, while OCD lesions retained cysts and erosions. Micro-CT analysis in percentage of bone volume fraction confirmed ESWT significantly improved bone regeneration compared to OCD at 12 weeks ($p < 0.05$, two-tailed paired *t*-test), suggesting that ESWT enhances bone formation and remodelling (Figure 1d).

ESWT reduced fibrotic protein type I collagen and improved the expression of type II collagen in OCD lesion

Immunostaining for collagen types I and II in drilling wound tissues revealed notable findings (Figures 2a and 2b). In addition to showing collagen type I and II expressions in Sham group, type I collagen was consistently present on the surface layers of reparative tissues in both OCD and ESWT groups between two and 12 weeks, with a gradual decline in the ESWT group at eight and 12 weeks ($p < 0.05$, two-tailed paired *t*-test) (Figure 2a). Conversely, type II collagen was absent in the OCD group throughout the experiment, but prominently expressed in the ESWT group at 12 weeks (Figure 2b). The results suggest that ESWT enhances type II collagen expression and promotes cartilage regeneration in OCD lesions.

ESWT stimulated the pivotal transcription factor SOX9 and aggrecan expression in OCD lesion

SOX9 is a well-known regulator of extracellular matrix proteins, including type II collagen and aggrecan, and its expression serves as supportive evidence for the chondrogenic effect. In the experiments, the Sham group exhibited the highest expression of SOX9 and aggrecan (Figures 2c and 2d), while no detectable SOX9 and aggrecan expression was observed in the OCD and ESWT groups at two, four, and eight weeks. However, at 12 weeks, the ESWT group ($p < 0.05$, two-tailed paired *t*-test) exhibited significantly higher expressions of SOX9 and aggrecan in the reparative tissues compared with the OCD group.

Wound healing process for regeneration of articular cartilage after ESWT on OCD lesion

In the previous results, ESWT on OCD lesions could promote both articular cartilage and subchondral bone regeneration faster than OCD lesion. The fibre and collagen arrangements and chondrocyte morphologies were presented to show the wound healing process by ESWT on OCD lesions (Figure 3). In Figure 3a, the images of HE staining at all timepoints were inspected and the regions of interest (ROIs) were indicated. Compared with the mature chondrocytes presented in the Sham group, the magnified areas showed that the OCD lesions evolved from fibrous cells to early chondrocytes in the colour devolution column. Upon comparison with the arcus collagen fibres in the Sham group, the magnified regions revealed a transition in the OCD lesions: from linear collagen fibres aligned horizontally to arcus collagen fibres aligned perpendicularly in the fibre/collagen orientation column. As a result, the threshold column indicated a gradual reduction in thread-like fibrous cells over time.

Figure 3b illustrates the progression of wound healing in the ESWT group based on data from Figures 1c and 1d, and Figure 2. In summary, flat and elongated fibroblasts align horizontally, and rapidly form a fibrous tissue layer two weeks after ESWT, a result of haematoma formation and fibrin clotting. By the fourth week, this layer thickens, facilitating fibroblast growth in less horizontal directions. At eight weeks, the reparative tissue exhibits fibrochondrocytic features with oval-shaped cells embedded in a fibrous matrix, aligned in circular orientations. By the twelfth week, chondroblasts or early chondrocytes develop, expressing SOX9, type II collagen, aggrecan, and proteoglycans. The tissue morphology demonstrates circular-oblique alignments. These results provide a detailed description of hyaline cartilage regeneration facilitated by ESWT in OCD lesions.

TGF-β and BMP-2 expression in OCD recovery following ESWT

We investigated the effect of ESWT on TGF-β and BMP-2 in both cartilage and subchondral bone marrow regions in relation to chondrogenesis and osteogenesis. TGF-β expression was significantly higher in the ESWT group compared to OCD at 12 weeks during chondrogenesis (Figure 4a), and ESWT also showed significant increases of TGF-β expressional intensity at four, eight, and 12 weeks in subchondral bone marrow (Figure 4b) compared to the OCD group. These results indicate that ESWT enhanced expression of TGF-β, supporting its positive effects on tissue regeneration.

In contrast, BMP-2 signals were extremely rare in OCD and ESWT groups at two, four, and eight weeks, while the Sham group exhibited BMP-2 signals in articular cartilage. However, at 12 weeks, ESWT displayed significant BMP-2 expression in chondrogenesis (Figure 4c). Furthermore, the ESWT group also showed significant increases of BMP-2 expressional intensity at four, eight, and 12 weeks in subchondral bone marrow (Figure 4c) than the OCD group ($p < 0.01$, two-tailed paired *t*-test). These findings suggest that ESWT promotes TGF-β and BMP-2 expressions, which may consequently contribute to chondrogenic and osteogenic recoveries, with particularly high levels at 12 weeks in the ESWT group compared to the OCD group (Figure 4).

Comparison of BMP-3, -4, -5, and -7 expression profiles in Sham, OCD, and ESWT groups

Here, we examined the expression levels of BMPs (BMP-3, -4, -5, and -7) in the Sham, ESWT, and OCD groups (Figures 5 and 6). In the hyaline cartilage of the Sham group, BMP-3 was present in chondrocytes. However, BMP-3 signals were rarely observed in both the OCD and ESWT groups at two, four, and eight weeks (Figure 5a). At 12 weeks, low but significant mean BMP-3 expression was detected in the cartilage of the ESWT group as compared with the OCD group (black arrows) ($p < 0.05$, two-tailed paired *t*-test). In addition, relative to the

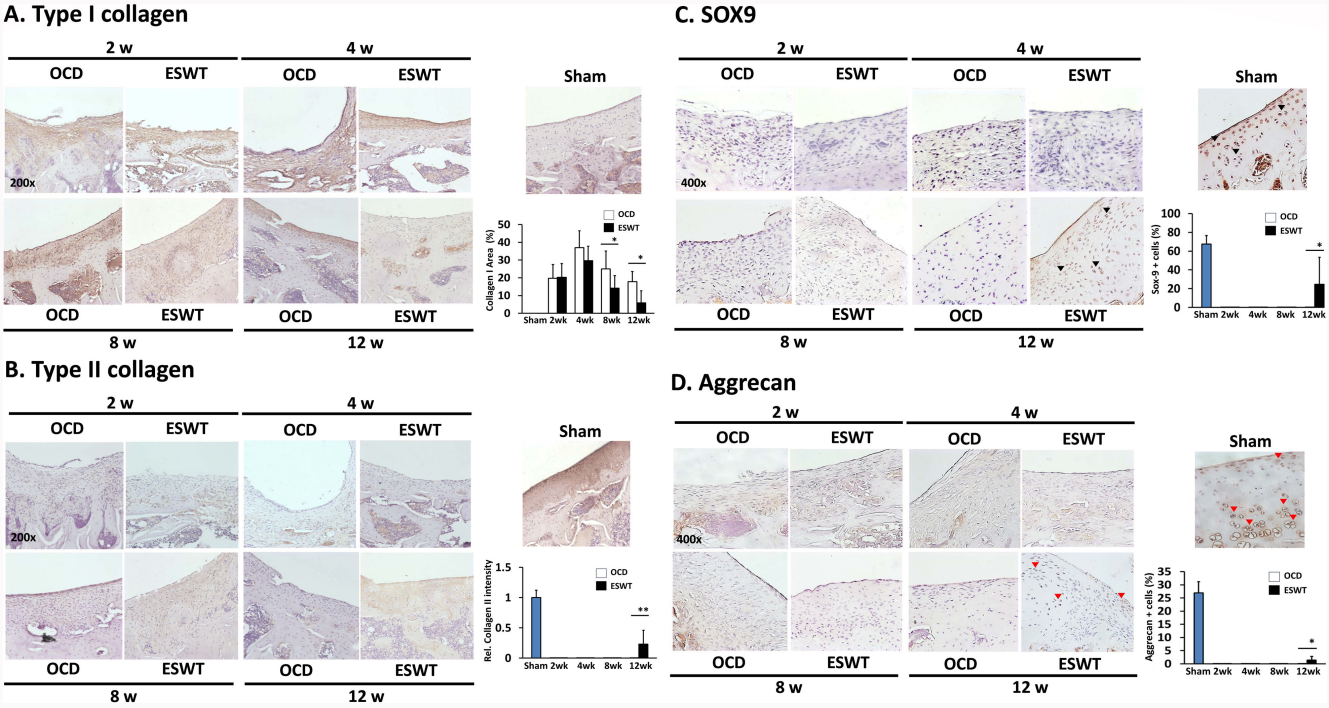

Fig. 2
The immunohistochemical (IHC) images and expression levels of type I collagen, type II collagen, SRY-box transcription factor 9 (SOX9), and aggrecan. a) type I collagen (×200 magnification), b) type II collagen (×200 magnification), c) SOX9 (×400 magnification), and d) aggrecan (×400 magnification) as well as the expression levels at two, four, eight, and 12 weeks. *p < 0.05 and **p < 0.01, comparing osteochondral defect (OCD) and extracorporeal shockwave therapy (ESWT) groups.

Sham group, the BMP-3 presented in bone marrow did not show significant differences when compared between OCD and ESWT groups (Figure 5b).

BMP-4, -5, and -7 exhibited expression levels in the cartilage layers of Sham group. Still, signals were rarely detected in both OCD and ESWT groups at two, four, and eight weeks. At 12 weeks, significant expressions of BMP-4, -5, and -7 were observed in the ESWT group, while infrequent signals were found in the OCD group, indicating that ESWT promoted their expression and chondrogenic recovery (Figure 5c, Figure 6a, and Figure 6c) ($p < 0.05$, two-tailed paired *t*-test).

In the subchondral bone marrow, the BMP-4 expressional intensity increased from two to four weeks and decreased from four to 12 weeks (Figure 5d). Both BMP-4 and BMP-5 levels were significantly higher in the ESWT group from two to 12 weeks compared to the OCD group (Figures 5d and 6b). The intensity of BMP-7 expression remained minimal until 12 weeks, when it was notably induced in the ESWT group, promoting bone regeneration more effectively than in the OCD group (Figure 6d).

These findings suggest that ESWT treatment enhances the expression of BMP-4, -5, and -7, potentially contributing to both cartilage and bone regeneration in OCD lesions.

Discussion

In our study, we investigated the effects of ESWT on the repair of hyaline cartilage and subchondral bone in rat knee lesions affected by OCD. Pathological changes in the damaged tissues were evaluated at two, four, eight, and 12 weeks after ESWT treatment, and compared with the OCD and Sham groups. Additionally, we analyzed the expression of fibrosis-related protein, type I collagen, as well as chondrogenic proteins including type II collagen, SOX9, and aggrecan, in the Sham, ESWT, and OCD groups. Furthermore, we measured the levels ofgrowth factors such as TGF-β and BMPs (including BMP-2, -3, -4, -5, and -7), which play a crucial role in improving hyaline cartilage and subchondral bone regeneration following ESWT in OCD lesions. Notably, our findings revealed a distinct pattern of improved articular cartilage regeneration after ESWT, characterized by a bottom-to-top and edge-to-centre progression (Supplementary Figure c). Moreover, the recovery of hyaline cartilage was observed following bone regeneration subsequent to ESWT treatment. Overall, our study provides comprehensive insights into the pathological changes and tissue recovery occurring in a rat model of OCD following ESWT.

OCD is a critical injury with a poor prognosis for conservative treatment in children and young people.[31] In addition, the available methods for OCD treatments have poor efficacy, and research efforts have rarely been committed to unravelling this issue in recent years. Subchondral drilling is widely used for small cartilage defects to stimulate the growth of new tissue and improve the symptoms of OCD; however, it may not be effective in all cases, and carries potential risks and complications such as infection, bleeding, and further damage to the joint.[32] Therefore, many clinical reports suggest general indications of the advantage of physical activity.[33] However, high-level evidence and basic studies are necessary to understand the mechanism and available strategies to improve the treatments and conservative management for stabilizing OCD lesions.

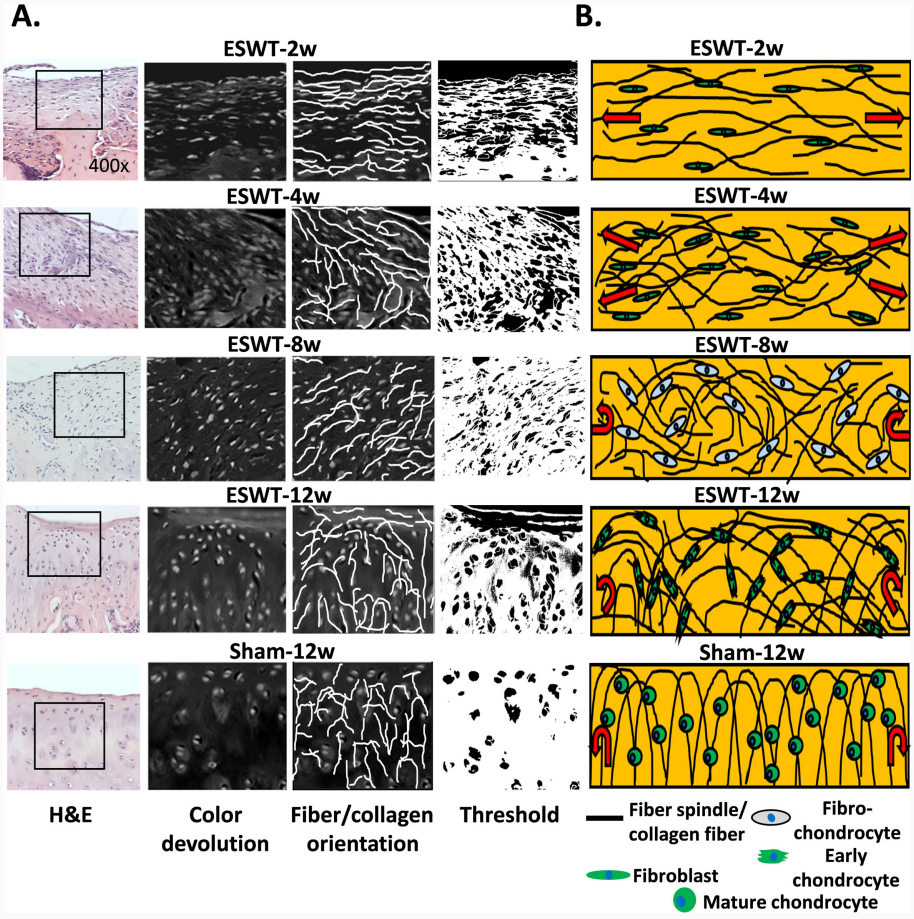

Fig. 3
The data demonstrate the regenerative dynamics of hyaline cartilage following extracorporeal shockwave therapy (ESWT) in osteochondral defect lesions over a two- to 12-week period. a) Assessment of cartilage conditions involves evaluating chondrogenesis (depicted through colour devolution columns) and collagen fibre alignment (represented by orientation and threshold columns). b) Schematic diagrams illustrate the processes of cartilage repair and chondrogenesis. H&E, haematoxylin and eosin.

The articular cartilage regeneration from the lesion is a critical step for OCD treatment. We know articular cartilage regeneration has a poor inherent ability for self-renewal. After the drilling injury, the repair process was initiated to improve the local matrix microenvironment and recruit fibrous cells into the injured sites, and immune cells were recruited in the damaged lining region (Figures 1b and 1c and Supplementary Figure c).[34,35] In the damaged region, type I collagen was rapidly induced by fibrotic cartilage to promote the repair of damaged tissue, leading to the formation of fibrotic tissue (Figure 2a).[36] In our study, ESWT demonstrated a significant decrease in the expression of type I collagen, suppression of fibrotic tissue formation, and reduced infiltration of immune cells. Furthermore, ESWT exhibited a positive effect by promoting the expression of type II collagen (Figure 2b). In addition, anabolic cytokines or growth factors such as TGF-β and BMPs can stimulate chondrocytes to synthesize and release matrix components required for tissue repair.[34,37] TGF-β/BMP signalling promotes chondrocyte proliferation, chondrogenic gene (*ACAN*, *SOX9,* and *COL2A1*) expression, and glycosaminoglycan protein (aggrecan, chondroitin sulphate, keratan sulphate, dermatan sulphate, and heparan sulphate) secretion.[37,38] Our study showed that ESWT had the ability to promote articular cartilage to self-renew after injury (Figure 3) and induced the expression of local matrix proteins, TGF-β, and BMPs, including BMP-2, -4, -5, and -7 (Figure 2d, Figure 5, and Figure 6).

A sprain or trauma can cause an OCD lesion, which is a state of damage to the articular cartilage and a subchondral bone disorder that can generate a free bone fragment. The severity of OCD and the treatment selection are influenced by the size and degree of detachment of the bone fragment.[39] Therefore, subchondral bone has been proposed as a precise therapeutic target for OCD treatment. In Zhang et al,[40] peripheral blood stem cells were implanted into the OCD subchondral bone, and the results demonstrated a significant improvement by MRI. In addition, scaffold-based treatments designed for localized growth factor delivery are often used for the bone regeneration of OCD in clinical and preclinical studies.[41,42] ESWT has been reported to improve the bone regeneration of OCD lesions in clinical trials and animal studies.[43] In addition, it has been reported that ESWT promotes YAP and TAZ signalling factors to contribute to bone and cartilage homeostasis as well as tissue regeneration.[44,45] ESWT promotes bone regeneration through mechanotransduction to stimulate the expression of growth factors such as TGF-β, BMP-2, and vascular endothelial growth factor (VEGF).[46,47] In this study, ESWT promoted the expression of TGF-β and BMPs in the subchondral bone marrow to improve bone regeneration. In addition, our results detail expression

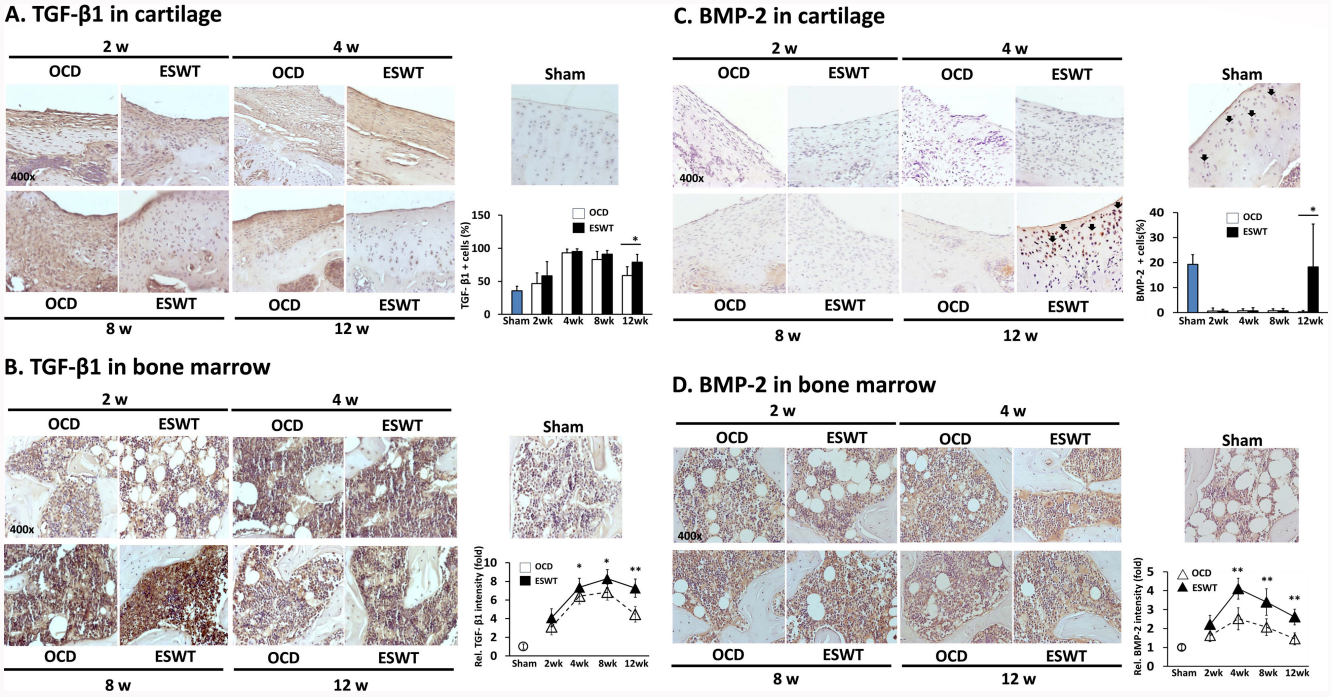

Fig. 4

The expression profiles of transforming growth factor (TGF)-β and bone morphogenetic protein (BMP)-2 in cartilage and in bone marrow of Sham, osteochondral defect (OCD), and extracorporeal shockwave therapy (ESWT) groups at the various time intervals. The histological section images show a) TGF-β in the cartilage; b) TGF-β in the bone marrow; c) BMP-2 in the cartilage; and d) BMP-2 in the bone marrow. All the images are presented at 400× magnification. In addition, the immunohistochemical stains are quantified as percentage of positive cells in the panels. *p < 0.05 and **p < 0.01 compared between the OCD and ESWT groups (two-tailed paired *t*-test).

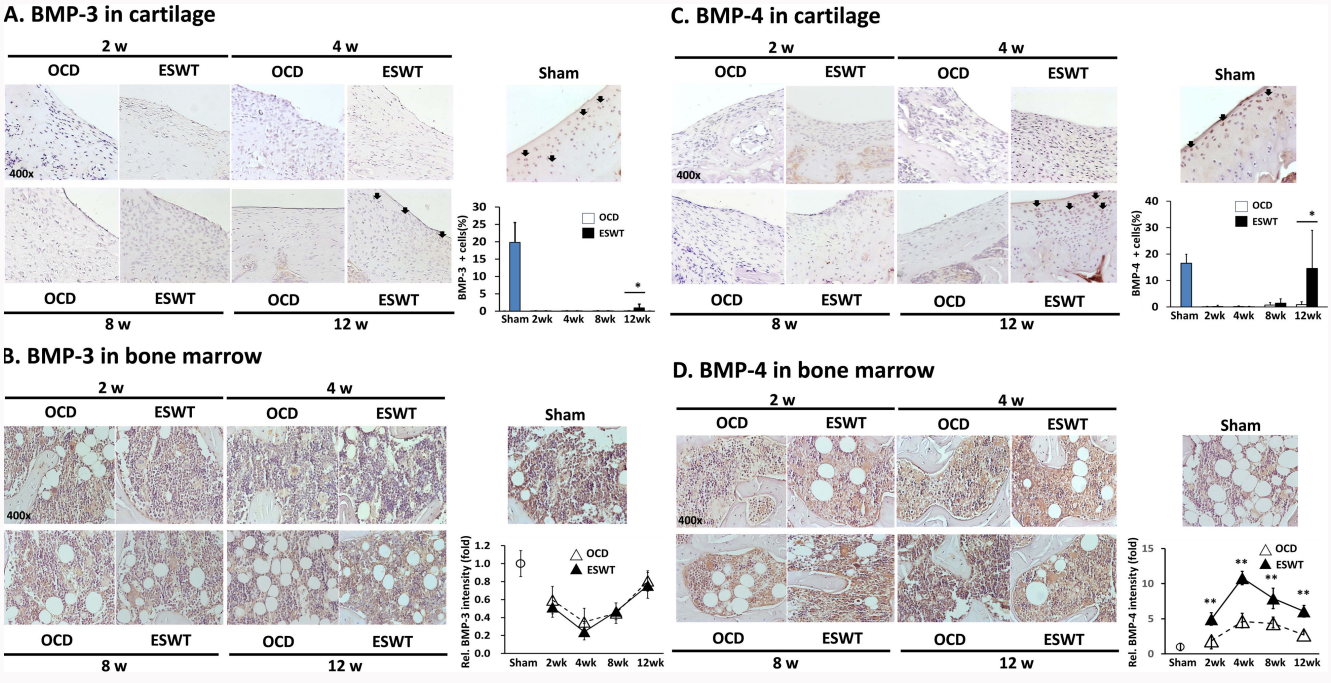

Fig. 5

The investigation shows the expression profiles of bone morphogenetic protein (BMP)-3 and BMP-4 in the cartilage and bone marrow of Sham, osteochondral defect (OCD), and extracorporeal shockwave therapy (ESWT) groups across various time intervals. Histological section images are presented to illustrate a) BMP-3 in the cartilage, b) BMP-3 in the bone marrow, c) BMP-4 in the cartilage, and d) BMP-4 in the bone marrow. All images are acquired at a magnification of 400×. Additionally, the quantification of immunohistochemistry stains involves determining the percentage of positive cells at the defect sites and assessing the intensity of bone marrow cells around the subchondral bone regions in the respective panels. *p < 0.05 and **p < 0.01, compared between the OCD and ESWT groups (two-tailed paired *t*-test).

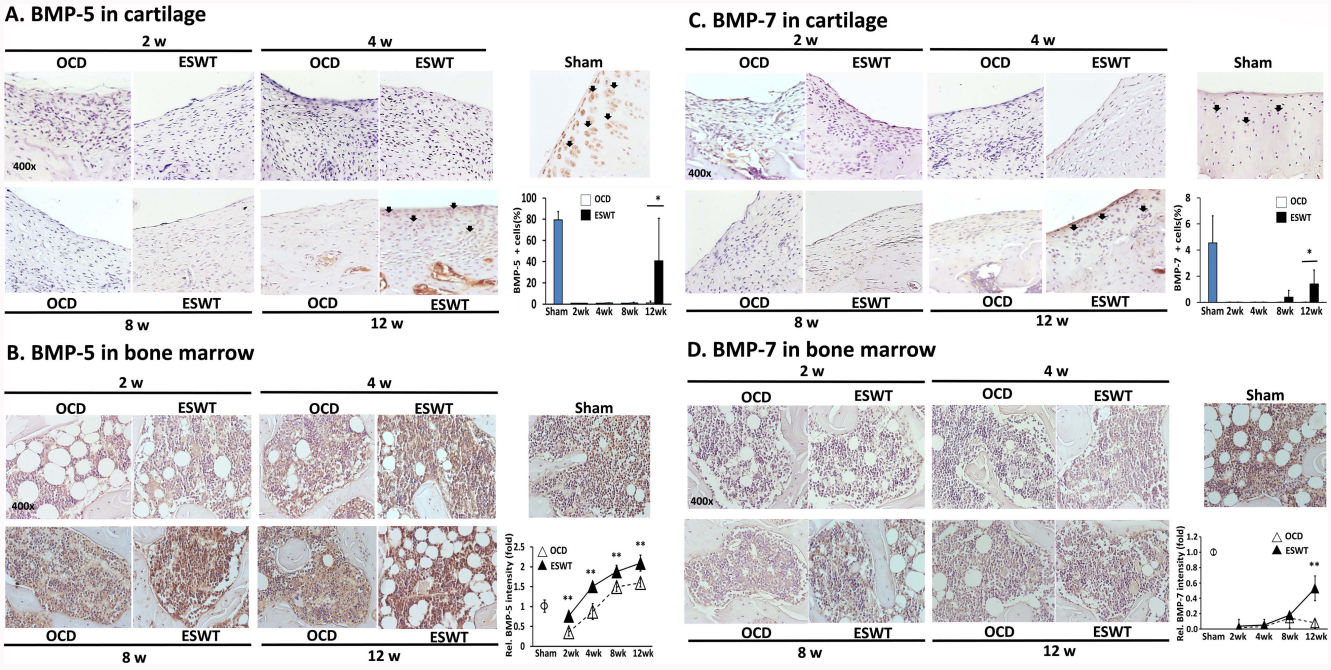

Fig. 6

The expression profiles of bone morphogenetic protein (BMP)-5 and BMP-7 in the cartilage and bone marrow of Sham, osteochondral defect (OCD), and extracorporeal shockwave therapy (ESWT) groups across various time intervals. Immunohistochemistry (IHC) images of BMP-5 expression are presented in a) the cartilage and b) the bone marrow, while images for BMP-7 expression are also taken from c) the cartilage and d) the bone marrow. All images were obtained at a magnification of 400×. The quantification of IHC stains includes the determination of the percentage of positive cells at the defect sites and the assessment of bone marrow cell intensity surrounding the subchondral bone regions in the respective panels. *p < 0.05 and **p < 0.01, compared between the OCD and ESWT groups (two-tailed paired *t*-test).

profiles of TGF-β, and BMP-2, -3, -4, -5, and -7 for bone and cartilage regeneration in OCD treatment after ESWT. Furthermore, several activities of pathways, including focal adhesion kinase (FAK), extracellular signal-regulated kinase 1/2 (ERK1/2), p38/mitogen-activated protein kinase (MAPK), and serine/threonine protein kinase B (AKT) are activated by ESWT for chondrogenesis and osteogenesis.[48] These data support the mechanism of ESWT for regeneration of OCD lesion.

In clinical practice, nonoperative treatment is usually attempted in patients with a stable OCD lesion because of its healing capacity, especially in lesions with an open physis.[49] However, the healing process of an OCD lesion is not always predictable, even if the patient quits sports activities and is immobilized for three to six months. In the existing literature, risk factors have been shown to predict the likelihood of healing, including lesion size, abnormal location, mechanical symptoms, and cyst-like lesions.[50,51] If a stable OCD lesion is not healed, it will gradually progress to an unstable lesion where surgical intervention is indicated.[52] The surgical approach usually ranges from simple subchondral drilling and fracture fixation to complicated osteochondral autograft transplantation.[53–55] Our animal study provides evidence supporting the use of ESWT as a potential treatment option to promote the healing of OCD in patients who prefer nonoperative methods.

The limitations of this study are as follows: it was performed using small animals, and therefore further investigation is needed through large animal or human clinical trials to confirm the results. The rat OCD lesion, as an induced injury, was used to investigate the molecular mechanism of ESWT, and its findings may not fully reflect the results observed in clinical treatments. Finally, there are various shockwave devices available on the market, and the optimal dosage for the treatment of OCD should be carefully determined and optimized through clinical trials.

In conclusion, this study demonstrates that in a rat OCD model, ESWT effectively reduces the formation of fibrotic tissue and stimulates the expression of growth factors including TGF-β, BMP2, -3, -4, and -5 during the early phase (2 to 4 weeks), promoting bone regeneration. Furthermore, the expression of BMP7 is significantly enhanced at 12 weeks following ESWT treatment compared to the OCD group. Moreover, throughout the process of hyaline cartilage regeneration, the ESWT group consistently exhibited higher expression levels of TGF-β from two to 12 weeks in comparison to the OCD group. Importantly, all BMPs contributed to the regeneration of articular cartilage with promotion of type II collagen, SOX9, and aggrecan, with the ESWT group demonstrating earlier progress at 12 weeks when compared to the OCD group. These findings suggest that ESWT has significant potential as a primary nonoperative treatment option, as it may prevent stable lesions from worsening, and promotes both bone and cartilage regeneration.

Supplementary material

Additional figures and tables.

References

1. **Dekker TJ**, **Aman ZS**, **DePhillipo NN**, **Dickens JF**, **Anz AW**, **LaPrade RF**. Chondral lesions of the knee: an evidence-based approach. *J Bone Joint Surg Am*. 2021;103-A(7):629–645.
2. **Krych AJ**, **Saris DBF**, **Stuart MJ**, **Hacken B**. Cartilage injury in the knee: assessment and treatment options. *J Am Acad Orthop Surg*. 2020;28(22): 914–922.
3. **Howell M**, **Liao Q**, **Gee CW**. Surgical management of osteochondral defects of the knee: an educational review. *Curr Rev Musculoskelet Med*. 2021;14(1):60–66.
4. **Hinckel BB**, **Thomas D**, **Vellios EE**, **et al**. Algorithm for treatment of focal cartilage defects of the knee: classic and new procedures. *Cartilage*. 2021;13(1_suppl):473S–495S.
5. **Zhang Z**, **Mu Y**, **Zhou H**, **Yao H**, **Wang D-A**. Cartilage tissue engineering in practice: preclinical trials, clinical applications, and prospects. *Tissue Eng Part B Rev*. 2023;29(5):473–490.
6. **Buck TMF**, **Lauf K**, **Dahmen J**, **Altink JN**, **Stufkens SAS**, **Kerkhoffs GMMJ**. Non-operative management for osteochondral lesions of the talus: a systematic review of treatment modalities, clinical- and radiological outcomes. *Knee Surg Sports Traumatol Arthrosc*. 2023;31(8): 3517–3527.
7. **Wang CJ**. An overview of shock wave therapy in musculoskeletal disorders. *Chang Gung Med J*. 2003;26(4):220–232.
8. **Wang CJ**. Extracorporeal shockwave therapy in musculoskeletal disorders. *J Orthop Surg Res*. 2012;7:11.
9. **Simplicio CL**, **Purita J**, **Murrell W**, **Santos GS**, **Dos Santos RG**, **Lana JFSD**. Extracorporeal shock wave therapy mechanisms in musculoskeletal regenerative medicine. *J Clin Orthop Trauma*. 2020;11(Suppl 3):S309–S318.
10. **Wang C-J**, **Wang F-S**, **Yang KD**, **et al**. Shock wave therapy induces neovascularization at the tendon-bone junction. A study in rabbits. *J Orthop Res*. 2003;21(6):984–989.
11. **Wang CJ**, **Wang FS**, **Yang KD**, **Weng LH**, **Sun YC**, **Yang YJ**. The effect of shock wave treatment at the tendon-bone interface-an histomorphological and biomechanical study in rabbits. *J Orthop Res*. 2005;23(2):274–280.
12. **Wuerfel T**, **Schmitz C**, **Jokinen LLJ**. The effects of the exposure of musculoskeletal tissue to extracorporeal shock waves. *Biomedicines*. 2022;10(5):1084.
13. **Huang X**, **Das R**, **Patel A**, **Nguyen TD**. Physical stimulations for bone and cartilage regeneration. *Regen Eng Transl Med*. 2018;4(4):216–237.
14. **Wang Q**, **Li ZL**, **Fu YM**, **et al**. Effect of low-energy shock waves in microfracture holes in the repair of articular cartilage defects in a rabbit model. *Chin Med J (Engl)*. 2011;124(9):1386–1394.
15. **Wang P**, **Liu C**, **Yang X-T**, **et al**. Effect of extracorporeal shock wave therapy on cartilage and subchondral bone remodeling in rabbits with ACLT-induced osteoarthritis. *Sichuan Da Xue Xue Bao Yi Xue Ban*. 2014;45(1):120–125.
16. **Benson BM**, **Byron CR**, **Pondenis H**, **Stewart AA**. The effects of radial shock waves on the metabolism of equine cartilage explants in vitro. *N Z Vet J*. 2007;55(1):40–44.
17. **Chou W-Y**, **Cheng J-H**, **Wang C-J**, **Hsu S-L**, **Chen J-H**, **Huang C-Y**. Shockwave targeting on subchondral bone is more suitable than articular cartilage for knee osteoarthritis. *Int J Med Sci*. 2019;16(1):156–166.
18. **Byron CR**, **Benson BM**, **Stewart AA**, **Stewart MC**. Effects of radial shock waves on membrane permeability and viability of chondrocytes and structure of articular cartilage in equine cartilage explants. *Am J Vet Res*. 2005;66(10):1757–1763.
19. **Ertürk C**, **Altay MA**, **Özardali İ**, **Altay N**, **Çeçe H**, **Işikan UE**. The effect of extracorporeal shockwaves on cartilage end-plates in rabbits: a preliminary MRI and histopathological study. *Acta Orthop Traumatol Turc*. 2012;46(6):449–454.
20. **Väterlein N**, **Lüssenhop S**, **Hahn M**, **Delling G**, **Meiss AL**. The effect of extracorporeal shock waves on joint cartilage--an in vivo study in rabbits. *Arch Orthop Trauma Surg*. 2000;120(7–8):403–406.
21. **Chu CH**, **Yen YS**, **Chen PL**, **Wen CY**. Repair of articular cartilage in rabbit osteochondral defects promoted by extracorporeal shock wave therapy. *Shock Waves*. 2015;25(2):205–214.
22. **Wen CY**, **Chu CH**, **Yeh KT**, **Chen PL**. *The Effect of Extracorporeal Shock Wave Therapy on the Repair of Articular Cartilage*. Hannemann K, Seiler F, eds. Springer, 2009: 881–885.
23. **Pineda S**, **Pollack A**, **Stevenson S**, **Goldberg V**, **Caplan A**. A semiquantitative scale for histologic grading of articular cartilage repair. *Acta Anat (Basel)*. 1992;143(4):335–340.
24. **Wakitani S**, **Goto T**, **Pineda SJ**, **et al**. Mesenchymal cell-based repair of large, full-thickness defects of articular cartilage. *J Bone Joint Surg Am*. 1994;76-A(4):579–592.
25. **Pfeifer CG**, **Kinsella SD**, **Milby AH**, **et al**. Development of a large animal model of osteochondritis dissecans of the knee: a pilot study. *Orthop J Sports Med*. 2015;3(2):2325967115570019.
26. **Cheng J-H**, **Chou W-Y**, **Wang C-J**, **et al**. Pathological, morphometric and correlation analysis of the modified Mankin score, tidemark roughness and calcified cartilage thickness in rat knee osteoarthritis after extracorporeal shockwave therapy. *Int J Med Sci*. 2022;19(2):242–256.
27. **Cizkova K**, **Foltynkova T**, **Gachechiladze M**, **Tauber Z**. Comparative analysis of immunohistochemical staining intensity determined by light microscopy, ImageJ and QuPath in placental Hofbauer cells. *Acta Histochem Cytochem*. 2021;54(1):21–29.
28. **Crowe AR**, **Yue W**. Semi-quantitative determination of protein expression using immunohistochemistry staining and analysis: an integrated protocol. *Bio Protoc*. 2019;9(24):e3465.
29. **Chen Y**, **Yu Q**, **Xu C-B**. A convenient method for quantifying collagen fibers in atherosclerotic lesions by ImageJ software. *Int J Clin Exp Med*. 2017;10:14927–14935.
30. **Cash JL**, **Bass MD**, **Campbell J**, **Barnes M**, **Kubes P**, **Martin P**. Resolution mediator chemerin15 reprograms the wound microenvironment to promote repair and reduce scarring. *Curr Biol*. 2014;24(12):1406–1414.
31. **Masquijo J**, **Kothari A**. Juvenile osteochondritis dissecans (JOCD) of the knee: current concepts review. *EFORT Open Rev*. 2019;4(5):201–212.
32. **Gao L**, **Goebel LKH**, **Orth P**, **Cucchiarini M**, **Madry H**. Subchondral drilling for articular cartilage repair: a systematic review of translational research. *Dis Model Mech*. 2018;034280.
33. **Wood D**, **Davis DD**, **Carter KR**. Osteochondritis dissecans. *StatPearls Treasure Island (FL)*. 2022.
34. **Hu H**, **Liu W**, **Sun C**, **et al**. Endogenous repair and regeneration of injured articular cartilage: a challenging but promising therapeutic strategy. *Aging Dis*. 2021;12(3):886–901.
35. **Li M**, **Yin H**, **Yan Z**, **et al**. The immune microenvironment in cartilage injury and repair. *Acta Biomater*. 2022;140:23–42.
36. **Rim YA**, **Ju JH**. The role of fibrosis in osteoarthritis progression. *Life (Basel)*. 2020;11(1):3.
37. **Deng ZH**, **Li YS**, **Gao X**, **Lei GH**, **Huard J**. Bone morphogenetic proteins for articular cartilage regeneration. *Osteoarthritis Cartilage*. 2018;26(9): 1153–1161.
38. **Thielen NGM**, **van der Kraan PM**, **van Caam APM**. TGFβ/BMP signaling pathway in cartilage homeostasis. *Cells*. 2019;8(9):969.
39. **Anbari A**, **Yanke AB**, **Cole BJ**. Osteochondritis dissecans. CT Sports Doc. 2008. https://sports-doc.net/Publications/ch014-X4397.pdf (date last accessed 12 June 2024).
40. **Zhang S-Y**, **Xu H-H**, **Xiao M-M**, **et al**. Subchondral bone as a novel target for regenerative therapy of osteochondritis dissecans: a case report. *World J Clin Cases*. 2021;9(15):3623–3630.
41. **Ai C**, **Lee YHD**, **Tan XH**, **Tan SHS**, **Hui JHP**, **Goh J-H**. Osteochondral tissue engineering: Perspectives for clinical application and preclinical development. *J Orthop Translat*. 2021;30:93–102.
42. **Lemoine M**, **Casey SM**, **O'Byrne JM**, **Kelly DJ**, **O'Brien FJ**. The development of natural polymer scaffold-based therapeutics for osteochondral repair. *Biochem Soc Trans*. 2020;48(4):1433–1445.
43. **Thiele S**, **Thiele R**, **Gerdesmeyer L**. Adult osteochondritis dissecans and focussed ESWT: a successful treatment option. *Int J Surg*. 2015;24(Pt B): 191–194.
44. **Li H-X**, **Zhang Z-C**, **Peng J**. Low-intensity extracorporeal shock wave therapy promotes recovery of sciatic nerve injury and the role of mechanical sensitive YAP/TAZ signaling pathway for nerve regeneration. *Chin Med J (Engl)*. 2021;134(22):2710–2720.
45. **Zhao Z**, **Wang Y**, **Wang Q**, **et al**. Radial extracorporeal shockwave promotes subchondral bone stem/progenitor cell self-renewal by activating YAP/TAZ and facilitates cartilage repair in vivo. *Stem Cell Res Ther*. 2021;12(1):19.
46. **Cheng J-H**, **Wang C-J**. Biological mechanism of shockwave in bone. *Int J Surg*. 2015;24(Pt B):143–146.

47. **d'Agostino MC**, **Craig K**, **Tibalt E**, **Respizzi S**. Shock wave as biological therapeutic tool: from mechanical stimulation to recovery and healing, through mechanotransduction. *Int J Surg*. 2015;24(Pt B):147–153.
48. **Mittermayr R**, **Haffner N**, **Feichtinger X**, **Schaden W**. The role of shockwaves in the enhancement of bone repair - from basic principles to clinical application. *Injury*. 2021;52 Suppl 2:S84–S90.
49. **Kocher MS**, **Tucker R**, **Ganley TJ**, **Flynn JM**. Management of osteochondritis dissecans of the knee. *Am J Sports Med*. 2006;34(7):1181–1191.
50. **Krause M**, **Hapfelmeier A**, **Möller M**, **Amling M**, **Bohndorf K**, **Meenen NM**. Healing predictors of stable juvenile osteochondritis dissecans knee lesions after 6 and 12 months of nonoperative treatment. *Am J Sports Med*. 2013;41(10):2384–2391.
51. **Uppstrom TJ**, **Haskel JD**, **Gausden EB**, **et al**. Reliability of predictive models for non-operative healing potential of stable juvenile osteochondritis dissecans knee lesions. *Knee*. 2016;23(4):698–701.
52. **Chambers HG**, **Shea KG**, **Anderson AF**, **et al**. Diagnosis and treatment of osteochondritis dissecans. *J Am Acad Orthop Surg*. 2011;19(5):297–306.
53. **Heyworth BE**, **Edmonds EW**, **Murnaghan ML**, **Kocher MS**. Drilling techniques for osteochondritis dissecans. *Clin Sports Med*. 2014;33(2):305–312.
54. **Bradley KE**, **Allahabadi S**, **Jansson HL**, **Pandya NK**. Outcomes of bioabsorbable fixation in the treatment of osteochondral lesions of the knee in adolescent patients. *Knee*. 2022;37:180–187.
55. **Gudas R**, **Gudaite A**, **Pocius A**, **et al**. Ten-year follow-up of a prospective, randomized clinical study of mosaic osteochondral autologous transplantation versus microfracture for the treatment of osteochondral defects in the knee joint of athletes. *Am J Sports Med*. 2012;40(11):2499–2508.

Author information

J-H. Cheng, PhD, Associate Research Fellow,
Center for Shockwave Medicine and Tissue Engineering, Kaohsiung Chang Gung Memorial Hospital and Chang Gung University College of Medicine, Kaohsiung, Taiwan;
Department of Medical Research, Kaohsiung Chang Gung Memorial Hospital and Chang Gung University College of Medicine, Kaohsiung, Taiwan;
Department of Leisure and Sports Management, Cheng Shiu University, Kaohsiung, Taiwan.

S-W. Jhan, MD, Attending Physician
S-L. Hsu, MD, Attending Physician
C-J. Wang, MD, Professor, Attending Physician
W-Y. Chou, MD, Attending Physician
K-T. Wu, MD, Attending Physician
Center for Shockwave Medicine and Tissue Engineering, Kaohsiung Chang Gung Memorial Hospital and Chang Gung University College of Medicine, Kaohsiung, Taiwan; Department of Orthopedic Surgery, Kaohsiung Chang Gung Memorial Hospital and Chang Gung University College of Medicine, Kaohsiung, Taiwan.

P-C. Chen, MD, Attending Physician, Department of Physical Medicine and Rehabilitation, Kaohsiung Chang Gung Memorial Hospital, College of Medicine, Chang Gung University, Kaohsiung, Taiwan.

D. Moya, MD, Professor, Attending Physician, Buenos Aires British Hospital, Buenos Aires, Argentina.

Y-N. Wu, PhD, Professor, School of Medicine, Fu Jen Catholic University, New Taipei City, Taiwan.

C-Y. Huang, MS, Research Assistant, Center for Shockwave Medicine and Tissue Engineering, Kaohsiung Chang Gung Memorial Hospital and Chang Gung University College of Medicine, Kaohsiung, Taiwan; Department of Medical Research, Kaohsiung Chang Gung Memorial Hospital and Chang Gung University College of Medicine, Kaohsiung, Taiwan.

Author contributions

J-H. Cheng: Conceptualization, Funding acquisition, Investigation, Project administration, Writing – original draft, Writing – review & editing.
S-W. Jhan: Formal analysis, Methodology.
P-C. Chen: Data curation, Methodology.
S-L. Hsu: Data curation, Methodology.
C-J. Wang: Writing – original draft, Writing – review & editing.
D. Moya: Writing – original draft.
Y-N. Wu: Formal analysis, Methodology.
C-Y. Huang: Data curation, Methodology, Writing – original draft.
W-Y. Chou: Conceptualization, Methodology, Supervision, Writing – review & editing.
K-T. Wu: Conceptualization, Funding acquisition, Investigation, Project administration, Writing – original draft, Writing – review & editing.

J-H. Cheng and K-T. Wu contributed equally to this work.

Funding statement

The authors disclose receipt of the following financial or material support for the research, authorship, and/or publication of this article: the funding sources were the Ministry of Science and Technology, Taiwan (MOST 109-2314-B-182A-037) and the Chang Gung Medical Foundation (CRRPG8J0041, CRRPG8J0042, CRRPG8J0043, CMRPG8J1591, and CLRPG8E0131).

ICMJE COI statement

The authors declare no conflicts of interest.

Data sharing

The data supporting the findings of this study are available within the article and its supplementary information files.

Acknowledgements

We are grateful to the Department of Medical Research, Kaohsiung Chang Gung Memorial Hospital, for supporting this work.

Ethical review statement

Rat maintenance and experimental procedures were approved by the Kaohsiung Chang Gung Memorial Hospital Animal Ethical and Care Committee (Approval Number: 2017111401). All studies are carried out in compliance with the ARRIVE guidelines.

Open access funding

This study was supported by the Ministry of Science and Technology, Taiwan (MOST 109-2314-B-182A-037) and the Chang Gung Medical Foundation (CRRPG8J0041, CRRPG8J0042, CRRPG8J0043, CMRPG8J1591, and CLRPG8E0131).